Wave trains in an excitable FitzHugh-Nagumo model: Bistable dispersion relation and formation of isolas

Georg Röder,* Grigory Bordyugov, and Harald Engel
Institut für Theoretische Physik, Technische Universität Berlin, Hardenbergstrasse 36, 10623 Berlin, Germany

Martin Falcke
Abteilung für Theoretische Physik, Hahn-Meitner-Institut, Glienicker Strasse 100, 14109 Berlin, Germany
(Received 21 September 2006; published 2 March 2007)

We investigate the dispersion relations of nonlinear periodic wave trains in excitable systems which describe the dependence of the propagation velocity on the wavelength. Pulse interaction by oscillating pulse tails within a wave train leads to bistable wavelength bands, in which two stable and one unstable wave train coexist for the same wavelength. The essential spectra of the unstable wave trains exhibit a circle of eigenvalues with positive real parts which is detached from the imaginary axis. We describe the destruction of the bistable dispersion curve and the formation of isolas of wave trains in a sequence of transcritical bifurcations unfolding into pairs of saddle-node bifurcations. It turns out that additional dispersion curves of unstable wave trains play an important role in the destruction of the bistable dispersion curve.

DOI: 10.1103/PhysRevE.75.036202 PACS number(s): 05.45.−a, 82.40.Bj, 82.40.Ck

I. INTRODUCTION

Excitation waves are observed in various physical, biological, and chemical systems such as catalytic surface reactions, neurons, cardiac muscle tissue, intracellular Ca^{2+} dynamics, and autocatalytic chemical reactions [1–5].

Traveling waves in one spatial dimension occur as solitary pulses or wave trains. Periodic wave trains are characterized by a dispersion relation, which describes the dependence of the propagation velocity c on the wavelength L. We call an increase of velocity with increasing wavelength normal dispersion, whereas anomalous dispersion is a decrease of velocity with increasing wavelength. In the case of normal dispersion [compare Fig. 1(a)] the solitary pulse is the fastest one. Wave trains with a finite wavelength propagate at a smaller velocity due to partial inhibition by the wake of the preceding pulse. There are nonmonotonic dispersion relations with a maximum velocity at a finite wavelength which leads to attractive pulse interaction within a wave train or a pulse pair [6–9]. Systems with oscillating dispersion curves [Fig. 1(b)] exhibit coexisting free spiral waves of different wavelengths [10] and particlelike traveling front deformations that mediate transitions within stable bound pulse pairs [11].

Recently, it was shown that the Oregonator model, which describes the Belousov-Zhabotinsky reaction, comprises in addition to an oscillatory dispersion a multivalued dispersion. Different stable wave trains coexist for the same wavelength [12]. Another type of multivalued dispersion was found in a model for intracellular Ca^{2+} waves [13]. The occurrence of a velocity gap in this dispersion destroys all periodic patterns which would have wavelengths within the gap.

The present work is a numerical case study of the FitzHugh-Nagumo (FHN) model in one dimension, which is a generic reaction-diffusion model for excitable media. It is well known that the model reproduces monotonic and oscillatory dispersion curves (Fig. 1); see also Ref. [14]. Here, we demonstrate the existence and describe the destruction of a bistable dispersion curve. The destruction entails the emergence of isolas of wave trains. The presence of other dispersion curves is found to be essential for the comprehensive understanding of the fragmentation of the bistable dispersion relation. The descriptions of wave trains is completed by a linear stability analysis.

The paper is structured as follows. Foremost we sketch basic features of the local FHN dynamics. We outline briefly the framework for the calculation of traveling waves and spectra of periodic wave trains. Then we present the bistable dispersion relation and discuss the stability of the corresponding wave trains. Finally we introduce additional dispersion curves that coexist with the bistable one and illustrate the fragmentation of the latter, which involves the emergence of isolas of wave trains.

II. MODEL AND METHODS

We consider a reaction-diffusion system in one spatial dimension with a fast activator u and a slow inhibitor v:

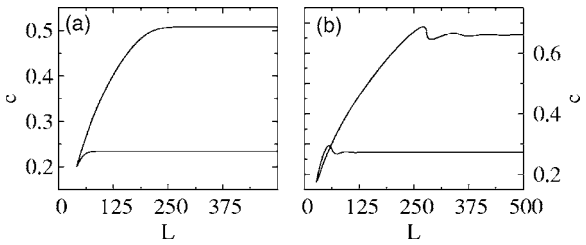

FIG. 1. Propagation velocity c of a periodic wave train vs wavelength L. The upper branch depicts (a) a monotonically increasing and (b) an oscillating dispersion relation, respectively. (a) $a=0.12$, (b) $a=0.02$; $b=0.25$, $\epsilon=0.3\times10^{-2}$. In both (a) and (b), the lower branch corresponds to unstable waves.

*Electronic address: roeder@mpipks-dresden.mpg.de

$$\frac{\partial}{\partial t}u = f(u,v) + \frac{\partial^2}{\partial x^2}u,$$

$$\frac{\partial}{\partial t}v = g(u,v). \tag{1}$$

The kinetics is given by the FHN equations

$$f(u,v) = -u(u-1)(u-a) - v,$$

$$g(u,v) = \epsilon(u - bv). \tag{2}$$

Parameter a adjusts the excitability. It is used as the main bifurcation parameter. The cubic and the linear nullcline $f(u,v)=0$ and $g(u,v)=0$, respectively, intersect in a unique stable fixed point of the local dynamics $(u,v)=(0,0)$ for our choice of $b=0.25$, $\epsilon=0.3\times10^{-2}$, and a close to zero. Upon decreasing a, the stable node turns into a stable focus and becomes unstable through a supercritical Hopf bifurcation at $a_{hb}=-\epsilon b$. The amplitude and period of the Hopf cycle blow up in a Canard explosion at $a_c<a_{hb}$ [15].

A periodic wave train and a solitary pulse of the reaction-diffusion equation (1) propagate with constant velocity c while maintaining their shape. They are stationary solutions in a comoving frame with coordinate $\xi=x-ct$. In particular, they correspond to a periodic orbit (wave train) and a homoclinic connection (solitary pulse) of the traveling wave ordinary differential equation (ODE)

$$\frac{d}{d\xi}\begin{pmatrix} u \\ v \\ w \end{pmatrix} = \begin{pmatrix} w \\ -\frac{1}{c}g(u,v) \\ -f(u,v) - cw \end{pmatrix}. \tag{3}$$

The eigenvalues of the fixed point $(u,v,w)=(0,0,0)$ determine the asymptotic behavior of the homoclinic connection. We consider a saddle focus with a pair of complex conjugate eigenvalues and one real eigenvalue. When a periodic orbit crosses a small neighborhood of the fixed point, those complex eigenvalues affect the periodic orbit, too.

To determine the stability of a periodic wave train $\vec{u}_c=(u_c(\xi),v_c(\xi))$ with wavelength L we add a small perturbation $\vec{u}(\xi,t)=\vec{u}_c(\xi)+\delta\vec{u}(\xi,t)$ and linearize the comoving frame reaction-diffusion equation. Using the separation ansatz $\delta\vec{u}(\xi,t)=e^{\lambda t}\vec{U}(\xi)$ we obtain the eigenvalue problem

$$\lambda\vec{U} = \mathcal{J}_{\vec{u}_c}\cdot\vec{U} + c\frac{d}{d\xi}\vec{U} + \mathcal{D}\frac{d^2}{d\xi^2}\vec{U} \tag{4}$$

with

$$\mathcal{J}_{\vec{u}_c(\xi+L)} = \mathcal{J}_{\vec{u}_c(\xi)}, \tag{5}$$

where $\mathcal{J}_{\vec{u}_c(\xi)}$ represents the Jacobian matrix of $(f(\vec{u}),g(\vec{u}))$ along the periodic wave train and $\mathcal{D}=\mathrm{diag}(1,0)$ the diffusion matrix. $\mathcal{J}_{\vec{u}_c(\xi)}$ is L periodic in ξ. The real part of λ is the growth rate of the eigenfunction $\vec{U}(\xi)$. The spectrum and the stability of a periodic wave train depend on the boundary conditions. The spectrum of an infinitely extended periodic wave train consists of the essential spectrum only [16]. A complex number λ belongs to the essential spectrum exactly if the eigenvalue equation (4) admits a solution on the interval $(0,L)$ with boundary conditions

$$(U,V,U_\xi)(L) = e^{i2\pi\gamma}(U,V,U_\xi)(0) \tag{6}$$

and a real $\gamma\in[0,1)$. The latter condition provides the existence of a solution of Eq. (4) that is a product of a long-wavelength factor $\exp[i(2\pi\gamma/L)\xi]$ and an L-periodic function.

If we confine the wave train in periodic boundary conditions, only certain points of the essential spectrum persist as eigenvalues. More precisely, a wave train with NL-periodic boundary conditions stands for $N=1,2,3,\ldots$ equally spaced high-amplitude excitations on a ring with perimeter NL. Allowed eigenfunctions are selected by $\gamma=0,1/N,2/N,\ldots,(N-1)/N$. Choosing proper values of γ, parametrized curves of the essential spectrum $\lambda(\gamma)$ provide stability informations for a wave train enclosed in NL-periodic boundary conditions. The Goldstone mode which is the derivative of the wave train with respect to ξ belongs to the eigenvalue $\lambda=0$ with $\gamma=0$.

We compute single pulses, periodic wave trains, and curves of the essential spectrum $\lambda(\gamma)$ of wave trains by a path following method using the software for continuation and bifurcation problems in ODEs AUTO [17,18]. Alternatively, applying L-periodic boundary conditions, we expand the functions $U(\xi)$ and $V(\xi)$ in the eigenvalue equation (4) in a finite number of Fourier modes. The resulting system of coupled linear equations for Fourier coefficients is solved using the standard package LAPACK.

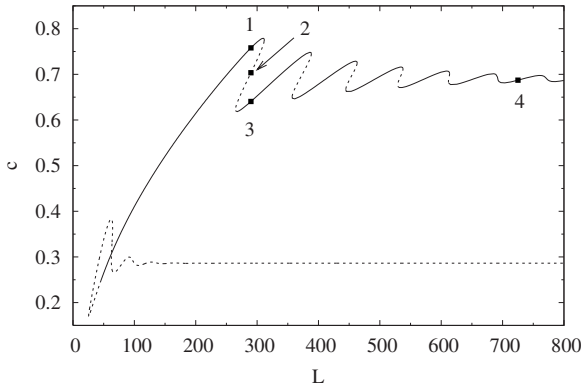

FIG. 2. Bistable dispersion relation. Solid (short-dashed) lines indicate stability (instability) of wave trains with L-periodic boundary conditions. Profiles of labeled waves are presented in Figs. 3 and 4. $a=0$, b and ϵ as in Fig. 1.

III. BISTABLE DISPERSION RELATION

In the traveling wave ODE (3), a solitary pulse is represented by a homoclinic connection to a fixed point, and periodic wave trains are represented by limit cycles. Thus, the problem of the existence of periodic wave trains in Eq. (1) and their dispersion relations is equivalent to the existence of branches of limit cycles in the traveling wave ODE (3). Wave trains plotted in Figs. 1 and 2 are represented by limit

cycles that converge to a homoclinic connection in the limit of large periods.

It is well known that, for large periods, the branch of limit cycles is strongly determined by the asymptotic properties of the approached homoclinic connection. For the case of a homoclinic connection to an equilibrium with a real leading eigenvalue (the closest to the imaginary axis), the branch of limit cycles in the "period-parameter" plane is monotonic, at least for large periods. If a pair of complex-conjugate eigenvalues are the leading eigenvalues, the branch of limit cycles approaches the limit in an oscillating manner [14,19]. For waves in reaction-diffusion systems this means that the dispersion curve for large L is determined by the decay behind the solitary pulse, since it is typically slower than the growth at the pulse front.

Decreasing the parameter a from 0.12 to 0.02, we detect a transition from monotonoic to oscillatory dispersion (see Fig. 1). In both cases there exists a well-defined limit for the velocity of wave trains for large wavelengths L. Each oscillation of the oscillatory dispersion relation adds a small-amplitude secondary maximum to the solution profile.

The oscillating dispersion relation of Fig. 1(b) turns into the multivalued dispersion relation of Fig. 2 by a sequence of pitchfork bifurcations. The bifurcation points are distinguished by the conditions

$$\frac{dL}{dc} = 0 \quad \text{and} \quad \frac{d^2L}{dc^2} = 0. \tag{7}$$

Each bifurcation results in the emergence of two further saddle node (SN) bifurcations, which are given by $dL/dc=0$ on the dispersion curve. These SN points confine a bistable wavelength band, where three solutions coexist. Two of them are stable and one is unstable. Simulation of the wave solutions of the reaction-diffusion equation (1) with periodic boundary conditions and variable domain size reveals hysteresis-type transitions between the two stable branches of wave trains. Note that there is only a finite number of bistability domains in the small-wavelength range.

Three coexisting wave trains for the same wavelength are depicted in Fig. 3. The high-amplitude pulse heads look similar for all three wave trains. The stable wave trains (labels 1 and 3 in Fig. 3) are distinguished by the number of the secondary maxima between two successive pulse heads. In the case of the unstable wave train (label 2 in Fig. 3), the secondary maximum is not completely developed. Following the dispersion curve to large wavelengths, the number of secondary maxima between successive pulse heads increases. Figure 4 illustrates the decay of the amplitude of the secondary maxima.

Let us now take a closer look at the stability of the coexisting wave trains with respect to the full reaction-diffusion system. Within our numerical accuracy we detect two kinds of instability points within a bistable wavelength band, namely, P points close to $dc/dL=0$ and SN points with $dL/dc=0$. Two sections of the dispersion relation of Fig. 2 which contain instability points are enlarged in Fig. 5. Curves of the essential spectrum are shown for selected wave trains. When we pass the upper P point by increasing the wavelength, a circle of eigenvalues flips from the left complex half plane to the right one. That circle captures all $\gamma \in [0,1)$. $\lambda=0$ holds for $\gamma=0$, i.e., the circle is attached to the origin of the complex plane. Following the dispersion curve and passing through the upper SN point, the circle of eigenvalues detaches from the origin. The circle remains in the right half plane until it attaches to the imaginary axis again at the lower SN point, and then flips to the left half plane at the lower P point. Beyond the bistable wavelength bands, the circle of eigenvalues does not detach from the imaginary axis in the right complex half plane. Computations of the discrete spectrum for L-periodic boundary conditions support the assumption that the described circle of eigenvalues is the only critical subset of the essential spectrum. We draw the follwing conclusions.

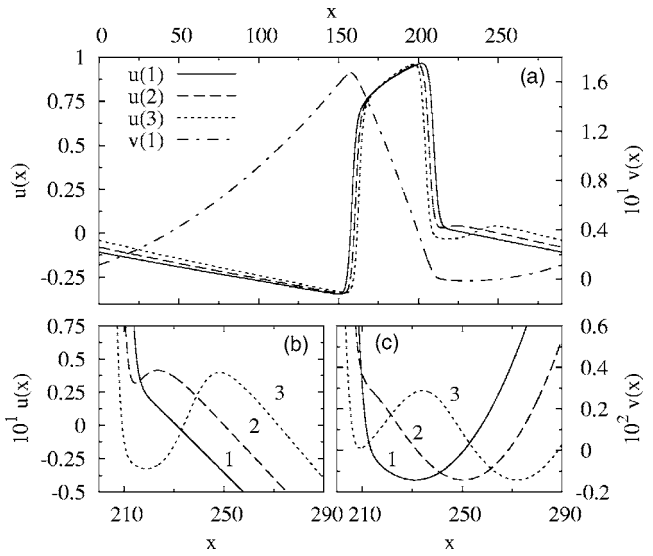

FIG. 3. Activator u and inhibitor v profiles along one wavelength $L=290$ (a). Propagation from left to right. Labels refer to those in Fig. 2. Appearance of a secondary maximum is enlarged in lower panels; for the activator in (b) and the inhibitor in (c). $a=0$; b and ϵ as in Fig. 1.

(i) Wave trains are stable with respect to arbitrarily large NL-periodic boundary conditions if we approach the first upper P point from small wavelengths, and in the regions be-

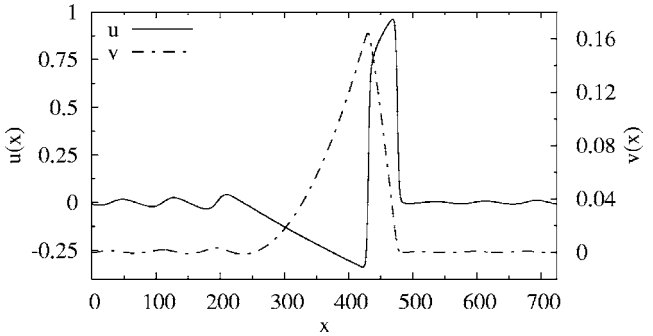

FIG. 4. Activator u and inhibitor v profile along one wavelength $L=725$ of label 4 in Fig. 2. Six secondary maxima of the profile correspond to six maxima of the dispersion relation counting from label 1 in Fig. 2. Propagation from left to right. $a=0$; b and ϵ as in Fig. 1.

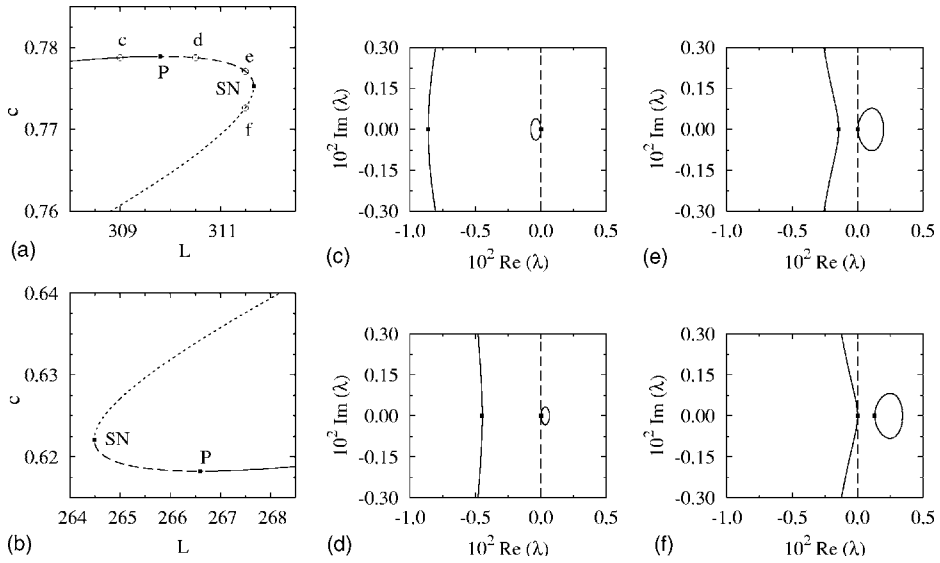

FIG. 5. Left panels (a) and (b) display enlargements of the bistable dispersion relation presented in Fig. 2. Solid (short-dashed) line indicates stable (unstable) wave trains with NL-periodic boundary conditions for all $N=1,2,3,\ldots$. Long-dashed line indicates stability for $N=1$ and instability for $N\geqslant 2$. Right panels (c)–(f) display subsets of essential spectra of pulse trains with reference to labels $c-f$ in (a). Squares indicate eigenvalues for $N=1$. Close to the P point a critical circle crosses the imaginary axis from left to right. We define the P point as the crossing of the eigenvalue belonging to $\gamma=0.5$. The circle detaches from the imaginary axis at the SN point. $a=0$; b and ϵ as in Fig. 1.

tween the lower and the upper P points of consecutive bistable wavelength bands.

(ii) Waves are stable for $N=1$ and unstable for $N\geqslant 2$ between P and SN points.

(iii) Waves are unstable for all N between the upper and the lower SN points of a bistability band.

(iv) Waves are stable for $N=1$ beyond all bistable wavelength bands. Stability (instability) for $N\geqslant 2$ is determined by the positive (negative) slope of the dispersion relation.

The width as well as the number of bistable wavelength bands increase with decreasing excitation parameter a. Bistability persists when the system passes through the Hopf bifurcation of the kinetics; however, we expect an additional instability for large wavelengths caused by the instability of the homogeneous stationary state [16]. Slightly below the Hopf bifurcation of the kinetics the traveling wave ODE (3) still possesses a homoclinic connection to the saddle focus.

In the following, the dispersion curve discussed so far will be referred to as the primary connected dispersion curve.

IV. EMERGENCE OF ISOLAS

We find the destruction of the primary connected dispersion curve upon decrease of the parameter a to values slightly above the Canard explosion of the local dynamics. Additional unstable wave trains play an important role in the destruction scenario.

In Figs. 6(a) and 6(b), two corresponding dispersion curves are shown, which exist in addition to the primary connected dispersion curve. We find again nonmonotonic curves displaying pronounced downward sawteeth. The left end point of the dispersion curve in Fig. 6(a) originates from a period-doubling bifurcation on the primary dispersion curve. Close to the end point, the u profiles of the waves have two maxima within one wavelength. One of these maxima disappears before label 1 is reached [see Fig. 6(a)]. The wave picks up a secondary maximum with each sawtooth passed through when we go along the dispersion curve from the small- to the large-wavelength range. This secondary maximum develops into a pulse head on the horizontal part of the dispersion curve following the sawtooth. The profile displays one pulse head and one secondary maximum at label 2, and two pulse heads and one secondary maximum at label 3. The dispersion curve in Fig. 6(b) is a closed curve in the (c,L) plane, a so-called isola. The corresponding u profiles exhibit one pulse head with two secondary maxima at label 4, and a sequence "pulse head, secondary maximum, pulse head, secondary maximum" at label 5. There exist even more dispersion curves which are not plotted. Some of them originate from period-doubling bifurcations on the primary dispersion curve. Parts of these curves consist of stable waves.

The primary connected dispersion curve is destroyed upon decreasing a in bifurcations which are collisions with dispersion curves like those shown in Fig. 6(a) and 6(b). The collision for the smallest wavelength happens first. All the other pictured collisions take place at the same smaller value of a (within our numerical accuracy). A new group of isolas emerges as a consequence of these bifurcations [Figs. 6(c) and 6(d)]. At the bifurcation point we have a transcritical bifurcation which unfolds into two saddle-node bifurcations. A comparison of the profile belonging to point 2 in Fig. 6(a) with the one of point 3 in Fig. 2 illustrates that profiles on the corresponding branches may become identical at the bifurcation point as required for a transcritical bifurcation. As a consequence of the transcritical bifurcation, a velocity gap for wave trains with secondary maxima opens up.

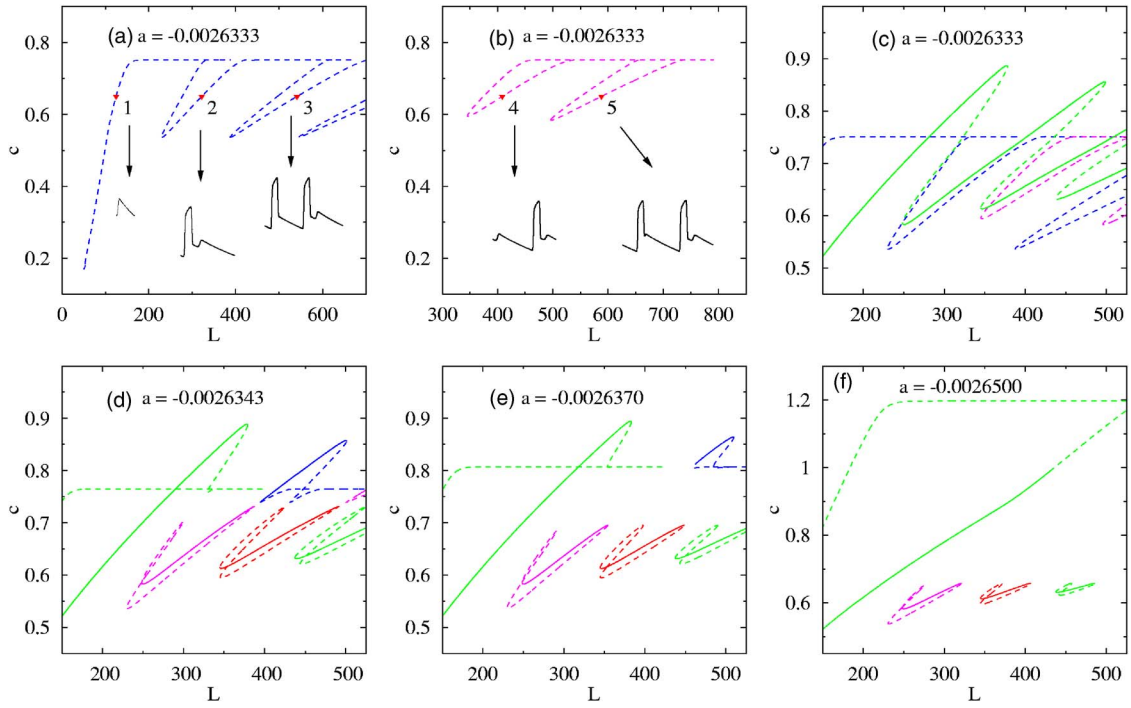

FIG. 6. (Color online) (a), (b) Additional dispersion curves and sketches of corresponding wave trains (activator profile) which are completely unstable. The dashed curve (blue online) in (a) arises from a period-doubling bifurcation at the primary dispersion curve. A small-amplitude maximum blows up along each plateau whereas a small-amplitude maximum develops within each sawtooth. The dashed curve in (b) (magenta online) is closed, a so-called isola. (c) Dashed curves of (a) and (b) (blue and magenta online) approach the primary dispersion (green online) before partial stable isolas separate. (d) Separated isolas and broken stable branches. A velocity gap opens up for wave trains with secondary maxima. (e) As isolas shrink the velocity gap expands. (f) Between isolas wavelength gaps open up. A solid (dashed) dispersion curve indicates stability (instability) of wave trains with L-periodic boundary conditions. b and ϵ as in Fig. 1.

Note that the first and second (counting from left to right) collisions occur between the primary connected dispersion curve and the curve in Fig. 6(a) while the third and fourth occur between the primary connected dispersion curve and the curve in Fig. 6(b). More dispersion curves have to be taken into account to describe the fragmentation of the primary connected dispersion curve at larger wavelengths.

Isolas first shrink and finally disappear, when a is decreased further as illustrated by Figs. 6(d)–6(f). As isolas shrink, the horizontal branch of the unstable dispersion curves shown in Figs. 6(a) and 6(b) shifts to larger velocity values. At parameter values close to the complete disappearance of isolas, the primary dispersion curve has been fragmented to such a degree that gaps in wavelength open up between isolas. Finally, all stable branches of the primary dispersion curve vanish but one [compare Fig. 6(f)].

V. CONCLUSION

Taking the FHN model as a representative example for excitable media, we study changes in the dispersion relation of periodic wave trains occurring under variation of an excitability parameter a. While normal dispersion is found for large values of a corresponding to excitable kinetics, anomalous dispersion with oscillating dispersion curves and finally bistable wavelength bands is obtained when the parameter a is decreased toward the Hopf bifurcation to oscillatory kinetics and slightly beyond.

The primary bistable dispersion curve is found to break up into disconnected fragments. We reveal the importance of so far undiscovered additional dispersion curves of unstable wave trains in this fragmentation. Transcritical collisions with the additional dispersion curves lead to the destruction of the primary one. The process results in the formation of *isolas* which represent closed segments of the dispersion curve. The stable wave trains of isolas display secondary maxima between pulse heads. In the small-wavelength region, however, there remains a large connected segment of the primary dispersion curve. The corresponding wave trains do not display secondary maxima.

Bistable dispersion resulting from pitchfork bifurcations was first reported in Ref. [12] and further studied in the context of the transition between phase and trigger waves in Ref. [20]. However, the formation of isolas and the existence of additional dispersion curves were not observed.

In accordance with the results for the Oregonator model we ascertain numerically a bistable dispersion relation of the FHN model close to the Hopf bifurcation of the local kinetics. Corresponding instability points (P and SN) within the bistable wavelength bands were found in both models. In distinction to the Oregonator results, here we describe a mechanism for the breakup of the primary bistable dispersion curve.

The discussed bifurcations of wave trains bear some similarity to the emergence of a dispersion gap in a model of intracellular Ca^{2+} dynamics [13] where a stable and an

unstable branch of disjunct dispersion curves collide. In this case, however, only one collision takes place and the two colliding curves are monotonic over a wide range of wavelengths. Consequently, a gap opens up representing forbidden velocities for which no periodic wave train exists.

Isola formation has been reported in the context of a nontransverse Shil'nikov-Hopf bifurcation [21]. Our scenario of isola formation is different since it involves several coexisting dispersion relations. However, some observations not in the focus of this paper indicate similarity with a scenario close to a nontransverse Shil'nikov-Hopf bifurcation. While decreasing the parameter a, we detected that the saddle-focus homoclinic connection merges with another homoclinic connection in a fold at $a=-0.002\,637\,3$. Both homoclinic connections are approached by periodic orbits, i.e., we have two wiggly curves in the (L,c) plane approaching (nearly) the same velocity c for large L. Collisions between both wiggly curves lead to isola formation at large wavelengths. That isola formation promises similarities with a case described in Ref. [21].

[1] M. C. Cross and P. C. Hohenberg, Rev. Mod. Phys. **65**, 851 (1993).
[2] A. S. Mikhailov, *Foundations of Synergetics I* (Springer-Verlag, Berlin, 1990).
[3] *Chemical Waves and Patterns*, edited by R. Kapral and K. Showalter (Kluwer Academic, Dordrecht, 1995).
[4] M. Falcke, Adv. Phys. **53**, 255 (2004).
[5] J. Keener and J. Sneyd, *Mathematical Physiology* (Springer-Verlag, Berlin, 1998).
[6] J. Christoph, M. Eiswirth, N. Hartmann, R. Imbihl, I. Kevrekidis, and M. Bär, Phys. Rev. Lett. **82**, 1586 (1999).
[7] M. Or-Guil, I. G. Kevrekidis, and M. Bär, Physica D **135**, 154 (2000).
[8] N. Manz, C. T. Hamik, and O. Steinbock, Phys. Rev. Lett. **92**, 248301 (2004).
[9] C. T. Hamik, N. Manz, and O. Steinbock, J. Phys. Chem. **105**, 6144 (2001).
[10] A. T. Winfree, Physica D **49**, 125 (1991).
[11] O. Steinbock, Phys. Rev. Lett. **88**, 228302 (2002).
[12] G. Bordiougov and H. Engel, Phys. Rev. Lett. **90**, 148302 (2003).
[13] M. Falcke, M. Or-Guil, and M. Bär, Phys. Rev. Lett. **84**, 4753 (2000).
[14] Y. A. Kuznetsov, *Elements of Applied Bifurcation Theory* (Springer, Berlin, 1995, 1998, 2004).
[15] M. Brons and K. Bar-Eli, J. Phys. Chem. **95**, 8706 (1991).
[16] B. Sandstede, in *Handbook of Dynamical Systems*, edited by B. Fiedler (Elsevier, Amsterdam, 2002), Vol. 2, p. 983.
[17] E. Doedel, R. Paffenroth, A. Champneys, T. Fairgrieve, Y. Kuznetsov, B. Oldeman, B. Sandstede, and X. Wang, Computer Code AUTO2000 (California Institute of Technology, Pasadena, CA, 2002).
[18] J. Rademacher, B. Sandstede, and A. Scheel (unpublished).
[19] P. Glendinning and C. T. Sparrow, J. Stat. Phys. **35**, 645 (1984).
[20] G. Bordiougov and H. Engel, Physica D **215**, 25 (2006).
[21] A. R. Champneys and A. J. Rodrígues-Luis, Physica D **128**, 130 (1999).